Multifrequency Radar Imagery And Characterization Of Hazardous And Noxious Substances At Sea

S. Angelliaume [(1)], B. Minchew [(2)], S. Chataing [(3)], Ph. Martineau [(1)] and V. Miegebielle [(4)]
[(1)] ONERA, France - [(2)] BAS, United Kingdom - [(3)] CEDRE, France - [(4)] TOTAL, France
Sebastien.Angelliaume@onera.fr

Abstract— **Maritime pollution by chemical products occurs at much lower frequency than spills of oil, however the consequences of a chemical spill can be more wide-reaching than those of oil. While detection and characterization of hydrocarbons have been the subject of numerous studies, detection of other chemical products at sea using remote sensing has been little studied and is still an open subject of research. To address this knowledge gap, an experiment was conducted in May 2015 over the Mediterranean Sea during which controlled releases of hazardous and noxious substances were imaged by an airborne SAR sensor at X- and L-band simultaneously.**
In this paper we discuss the experimental procedure and report the main results from the airborne radar imaging campaign.

Keywords—SAR, ocean, pollution, HNS, oil, multifrequency

I. INTRODUCTION

Airborne and spaceborne radar remote sensing is often used for oil slick detection over maritime surface, [1]-[3]. In an operational context, oil slicks are usually detected using synthetic aperture radar (SAR). Once detected, the spill is usually characterized using optical imagery [4]. Unlike hydrocarbons, there is limited research on hazardous and noxious substances (HNS) at sea using remote sensing. In that context, an experimental campaign of measurements (called POLLUPROOF) was conducted in May 2015 in the Mediterranean Sea. Controlled releases of six chemical and non-hydrocarbon oil products were carried out in collaboration with the French Navy and Customs. Polarimetric SAR (POLSAR) data were acquired at X- and L-band simultaneously by SETHI, the ONERA airborne SAR system [5], over released products. The aim of this work is first to study the capability of high resolution SAR imagery to detect HNS at sea and then to study the potential of radar imagery to quantify and characterize the spill.

II. EXPERIMENTATION AT SEA

A. Radar imagery

For the POLLUPROOF campaign, quad-pol SAR data have been acquired simultaneously at X- and L-band, with a resolution of 0.5 and 1.0 m, respectively. Incidence angle varies across the swath from 34° to 52°. Instrumental noise floor has been estimated using the method proposed in [6] and the results are shown Fig. 1. The Noise Equivalent Sigma^0 (NESZ) is very low, allowing sufficient Signal to Noise Ratio (SNR) over the spill for efficient analysis.

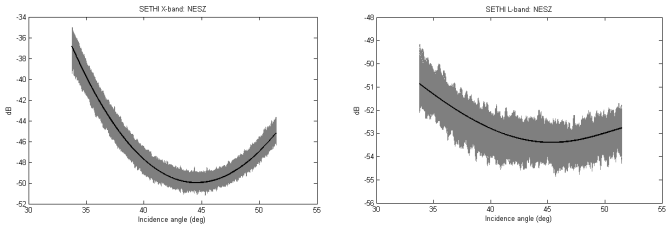

Fig. 1. SETHI - Instrumental noise at X-band (left) and L-band (right)

B. Chemical products

Six chemical substances have been chosen to evaluate the capability of radar sensors. The choice was made to cover different chemical families and be as representative as possible of chemical products often transported by sea and classified as noxious substances:

Toluene: toluene is a colorless liquid at ambient pressure and temperature, with a specific gravity of 0.867g.cm^{-3}. It is nearly insoluble in water (0.535g.L^{-1} at 25°C) and tends to evaporate relatively easily (vapor pressure of 2.91kPa at 20°C).

Heptane: at ambient pressure and temperature, heptane is a colorless liquid, volatile (6 to 7.7 kPa at 20°C) and nearly insoluble in water (< 2mg.L^{-1}). With a specific gravity of 0.710g.cm^{-3}, heptane is lighter than water and floats.

FAME: at ambient pressure and temperature, Fatty Acid Methyl Esters are a liquid with a specific gravity of 0.888g.cm^{-3}. It is pretty much insoluble in water (solubility of 0.023mg.L^{-1} at 20°C) and practically does not evaporate (vapor pressure of 0.42kPa at 25°C).

Methanol: methanol is a colorless liquid (specific gravity of 0.791g.cm^{-3}), volatile (vapor pressure of 12.3kPa at 20°C), miscible in water, inflammable and toxic.

Rapeseed Oil: rapeseed or colza oil is the second most consumed food oil in France. At ambient pressure and temperature, it is a viscous yellowish liquid with a specific gravity of 0.910g.cm^{-3}. Rapeseed oil is insoluble in water and does not evaporate (vapor pressure below 0.01kPa at 25°C).

Xylene: xylene or dimethylbenzene is a group of aromatic hydrocarbons. Its specific gravity of 0.87g.cm^{-3} makes it float on water. Xylene is slightly soluble in water (solubility below 20mg.L^{-1}) and is not likely to evaporate.

During the POLLUPROOF experiment, 1 m^3 of each of these products was released at sea and imaged by airborne radar sensors.

III. METHODOLOGY

A. Scattering from ocean surface

For the frequency bands mainly used in Earth Observation (X-, C- and L-band) and for incidence angles ranging from 30° to 60°, an ocean surface is a randomly rough surface where the radar backscatter is dominated by the Bragg scattering mechanism. As a consequence, the radar backscattered power, which is commonly defined by the normalized radar cross-section (NRCS), is greater in VV polarization than in HH and HV, [7]. For each polarization, the NRCS is proportional to the spectral energy density of the sea surface waves with wavelength (λ_{sea}) that satisfies:

$$\lambda_{sea} = \frac{\lambda_{EM}}{2\sin(\theta_i)} \tag{1}$$

where λ_{EM} and θ_i are the wavelength and the local incidence angle of the electromagnetic (EM) waves transmitted by the radar system, respectively.

Ocean surface is usually modeled as a composition of slightly rough tilted facets, each of which has superimposed small-scale surface roughness that creates a Bragg scatterer. Small-scale roughness is randomly distributed on the scattering surface and responds to the strength of local wind (i.e, gravity-capillarity waves). The tilt of the facet is caused by larger scale gravity waves on the ocean surface. The orientation of the facet normal in the radar reference frame is defined by two angles ψ and ξ. The resulting local incidence angle of the EM wave is:

$$\theta_i = \cos^{-1}\left[\cos(\theta+\psi)\cos\xi\right] \tag{2}$$

where θ is the EM angle of incidence relative to local, un-tilted up.

The sea may be modeled as the superposition of two independent processes describing the small and large scale components. Two-Scales Model (TSM), based on a spectral description of the sea surface, has been proposed to formulate this composite-surface scattering , [8]-[9]. The NRCS is then given by [7]:

$$\sigma^0_{pp} = 4\pi k^4_{EM}\cos^4\theta_i \Gamma_{pp} W \tag{3}$$

where the subscript *p* denotes either H or V polarization, $k_{EM} = 2\pi/\lambda_{EM}$ is the EM wavenumber, *W* is the spectral density of the ocean surface roughness and Γ_{pp} is the reflectivity defined by:

$$\Gamma_{pp} = \left| \left(\frac{\sin(\theta+\psi)\cos\xi}{\sin\theta_i} \right)^2 \alpha_{pp} + \left(\frac{\sin\xi}{\sin\theta_i} \right)^2 \alpha_{qq} \right|^2 \tag{4}$$

where the subscript *q* ($q \neq p$) denotes either H or V.

The Bragg scattering coefficients (α_{pp}, α_{qq}) only depend on the local incidence angle of the EM wave θ_i and the relative dielectric constant ε. Finally, for a given geometry of acquisition (fixed incidence angle) and assuming that the ocean surface is homogeneous over a sufficiently large area, the NRCS is only depending on the EM wavelength, the relative dielectric constant and the sea surface roughness.

In the case of an ocean surface covered by slicks, the product surface layer will dampen the capillarity waves, thereby attenuating the radar backscattered power by diminishing the surface roughness. The relative dielectric constant can also be modified in the case of a product which mixes with seawater. The resulting dielectric constant will be smaller than for pure seawater [10].

B. Detection and relative quantification

Many studies have suggested using POLSAR parameters to improve slicks detection capability (see review in [3]). A comprehensive comparison of those parameters was undertaken by [11]. Following [12], [11] quantitatively demonstrates the effectiveness of the *Polarization Difference* (PD=VV-HH in linear units) for slick detection on the ocean surface. The main drawback of the *Polarization Difference (PD)* is that it is not normalized, making it difficult to define a threshold with which a detection map can be established. To overcome this limitation, we propose a normalized variant of PD. We note that PD ranges from a maximum value (PD_{max}) that occurs in the case of a clean sea surface and goes to 0 as the impact of the substance on the surface increases. Hence, we define the *Normalized Polarization Difference (NPD)* as:

$$NPD = \frac{PD_{\max} - PD}{PD_{\max}} \qquad 0 \le NPD \le 1 \tag{5}$$

NPD is equal to 0 in the case of a clean sea surface and goes to 1 as the impact of the substance on the ocean surface increases. PD_{max} is the polarization difference value in the case of a clean sea surface and can be estimated through a physical two-scale model [9], [13] or an empirical model [14], using wind speed and wind direction information.

NPD can be interpreted as an indication of the presence and the impact of a substance on the ocean surface. It can be used directly or thresholded to produce a binary detection map.

C. Oil/water mixing index

The basic premise of the oil/water mixing index (M) is that radar backscattered power is diminished by oil slicks through mechanical damping of Bragg-wavelength capillary waves and reductions in the relative dielectric constant of the upper few centimeters near the sea surface [10], [15]. By decoupling the relative contribution to signal attenuation of surface waves mechanical damping and changes in dielectric constant, we can define the characteristics of the slick along a spectrum ranging from thin surface films to thicker emulsions. This information is critical for efficient cleanup operations.

As described in [10], the methodology can be summarized as:

1. Use the co-polarized ratio over uncontaminated seawater and an assumed value for the dielectric constant of pure seawater, ε_r^{water}, to infer the long-wavelength tilting of the ocean surface.

2. Calculate the short-wavelength roughness spectrum over uncontaminated water, W^{water}, by applying the tilt angles inferred in Step 1.
3. For each pixel of contaminated water, infer the local (effective) relative dielectric constant, ε_r^{oil}, from the co-polarized ratio and the inferred long-wavelength tilt angles deduced from Step 1.
4. Calculate the short-wavelength roughness spectrum over contaminated water, W^{oil}, using the dielectric constant inferred in Step 3 and the tilt angles obtained in Step 1.

M values can then be calculated as follows:

$$M = M_W - M_\alpha \quad (6)$$

$$M_W = \frac{W^{water} - W^{oil}}{W^{water}} \quad ; \quad M_\alpha = \frac{|\alpha_{VV}^{water}|^2 - |\alpha_{VV}^{oil}|^2}{|\alpha_{VV}^{water}|^2} \quad (7)$$

M_W is the *normalized damping factor* and M_α is the *normalized power attenuation factor*, both are ranging from 0 to 1. M_W is a measure of how much the product will attenuate the sea surface roughness; M_α is a measure of how much the backscattered signal is attenuated due to a decrease of the relative dielectric constant.
M is ranging from -1 to 1. Negative values indicate that the decreasing of the EM signal is more due to a decrease of the relative dielectric constant than to a decrease of the surface roughness; meaning that the product is mixed with the seawater. On the opposite, positive values indicate that the decreasing of the EM signal is mainly due to a smoothing of the ocean surface and thus we are in presence of a product that forms a film on the sea surface.

IV. Results and Discussion

A. Observation of Hazardous and Noxious Sustances at sea

Heptane and Toluene: both substances were never observed in SAR images, at X- and L-band; most likely because they are extremely volatile products, which do not impact the surface roughness. Please note that products (1 m^3 each) have been released only 5 and 10 min before SAR acquisitions.

Methanol and Xylene: as methanol is an extremely volatile substance soluble in the water column and as SAR acquisition began 40 min after the end of the release, methanol was never observed in SAR images. On the other side, the impact of xylene is clearly observable on X- and L-band SAR imagery.

Rapeseed oil and FAME: FAME and rapeseed oil are two persistent substances; which are both clearly observable on SAR images acquired at X- and L-band.
Figure 2 shows an illustration of VV polarized images acquired simultaneously at X- and L-band over the spill. From in situ information, we know that FAME is ranging from azimuth 4100 m to 5500 m, and that rapeseed oil is from azimuth 6000 m to 8500 m, and between we have a mixture of the two products. While it is not possible to visually distinguish the FAME and rapeseed oil, we observe a significant difference between L- and X-band acquisitions.

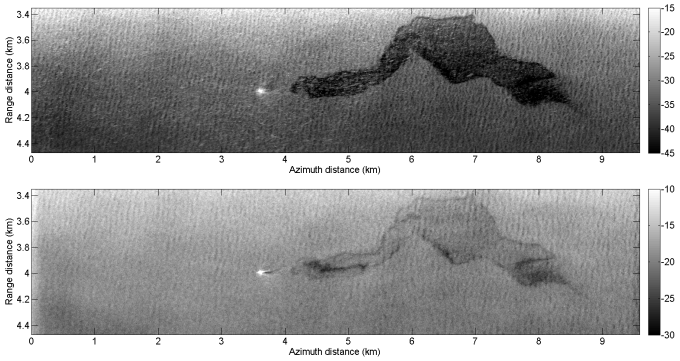

Fig. 2. X-VV (top) and L-VV (bottom) images over rapeseed oil and FAME

As expected, contrast between the spill and the clean sea surface is more significant at X- than at L-band. However, while at X-band the spill seems homogeneous, at L-band we observe strong variation of the EM signal into the spill with dark patches, due to a stronger impact of the HNS on the sea surface roughness at wavelengths corresponding to the L-band Bragg wavelength. As previously demonstrated by [16] or [17], it confirms that the EM signal backscattered by HNS is dependent on the wavelength and using different frequency bands should allow us to better characterize the spill.

B. Detection and quantification of impact on the sea surface

As presented in III.B, the *Normalized Polarization Difference (NPD)* can be used for detection of HNS at sea and quantification of their impact on the ocean surface.
The proposed method is divided into 2 steps: a detection mask is first calculated by thresholding the NPD map at X-band. Then, the detection mask is applied to the NPD map computed at L-band. Fig. 3 below shows NPD map at L-band, thresholded for values greater than 0.7 at X-band. We can observe that, first the spill is well identified using this automatic method; then, L-band can provide useful information for spill quantification and characterization.

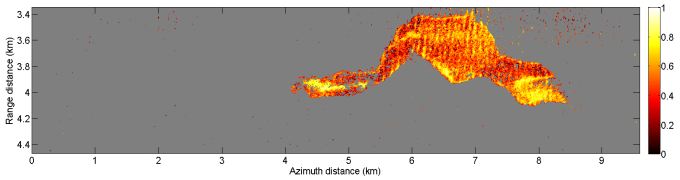

Fig. 3. L-band Normalized Polarization Difference - FAME and rapeseed oil

Hence, information provided by Normalized Polarization Difference and simultaneous use of two frequency bands, allow us to detect HNS at sea and to quantify their impact on the ocean surface in terms of roughness. However, results shown Fig. 3 do not enable us to distinguish between the two products that form the spill (rapeseed oil and FAME).

C. Characterization

In Fig. 2 and 3, spill is composed by two chemical products: the right part is rapeseed oil and the left part is FAME; in the middle there is a mixture of two. One can expect different behavior of each product on the sea surface: rapeseed oil is supposed to remain above the surface and produce a more or less homogeneous film. FAME will form a

cloud in the water column composed by micro-droplets. These behaviors must be recovered by SAR imagery as they impact the ocean surface in different ways: damping of capillarity waves and/or modification of the dielectric constant by mixing with sea water.

Following results presented above, we focus on L-band data and compute M_W, M_α and M parameters using the method presented in III.C. and initially published in [10] for the case of an oil-related incident. Fig. 4 shows the mixing index (M) map obtained over the full region of interest. We clearly observed the separation between the two products constituting the spill. As expected, surface is rougher over FAME than over rapeseed oil, the latter having more damped capillarity waves; moreover, mixing is more present over FAME than over rapeseed oil. As a consequence, FAME appears with negative M value and rapeseed oil with positive M value.

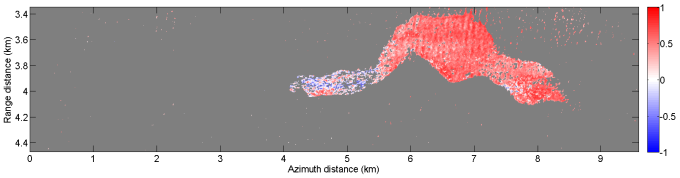

Fig. 4. L-band M parameter - FAME and rapeseed oil

V. Conclusion

Due to the increase of maritime transport of hazardous and noxious substances (HNS), controlling chemicals pollution at sea become crucial. As for oil spill, remote sensing is a great interest for detecting, quantifying and characterizing chemical product that was discharged. However, our knowledge on the ability of remote sensing to achieve thus is still limited.

An experimental campaign of acquisition (POLLUPROOF) has been conducted in May 2015 over the Mediterranean Sea during which controlled releases of HNS have been realized. Among the six products tested, three have been detected without any ambiguity using SAR imagery: rapeseed oil, FAME and xylene. For the three others, the non-detectability can be caused either by a high volatility of tested products or by an impact into the water column that physically does not affect the EM backscattered signal.

In this paper, an accurate method using X- and L-band radar imagery has been developed to detect and quantify the impact of chemical products at sea. X-band can easily detect spills, even when the impact on the surface is limited; L-band is then used to quantify this impact. A *Normalized Polarization Difference* (NPD) parameter is then introduced for this purpose. We showed that, at L-band, the NPD parameter takes a wide range of values within the spill; this variation is related to the impact of the product on the ocean surface. Then, we showed that the distinction between two HNS within the same spill is possible with radar imagery only. We conclude that, using SAR data with the suitable wavelength can allow us to define the characteristics of the slick along a spectrum ranging from thin surface films to thicker emulsions. This information is critical for efficient cleanup operations.

Acknowledgement

Research presented in this paper is part of the POLLUPROOF research program (ANR-13-ECOT-007) funded by the French National Research Agency (ANR).
Authors are very grateful to everyone involved in the experiment at sea; to G. Soriano and C.-A. Guerin for GO-SSA modeling and to P. Dubois-Fernandez and H. Oriot from ONERA for successful discussions.

References

[1] Brekke, C.; Solberg, A. H. S., "Oil spill detection by satellite remote sensing". *Remote Sensing of Environment.* ISSN 0034-4257. *95*(1), s 1-13, 2005.

[2] Girard-Ardhuin, F.; Mercier, G.; Collard, F.; Garello, R., "Operational oil-slick characterization by SAR imagery and synergistic data," IEEE J. Ocean. Eng., vol. 30, no. 3, pp. 487–495, Jul. 2005.

[3] Solberg, AH.S., "Remote Sensing of Ocean Oil-Spill Pollution," *Proceedings of the IEEE* , vol.100, no.10, pp.2931,2945, 2012.

[4] Leifer I. & al., "State of the art satellite and airborne marine oil spill remote sensing: Application to the BP Deepwater Horizon oil spill", Remote Sensing of Environment, 2012.

[5] Bonin, G. *et al.*, "The new ONERA multispectral airborne SAR system in 2009," *Radar Conference, 2009 IEEE*, Pasadena, CA, 2009, pp. 1-3.

[6] Hajnsek, I.; Pottier, E.; Cloude, S.R., "Inversion of surface parameters from polarimetric SAR," *Geoscience and Remote Sensing, IEEE Transactions on* , vol.41, no.4, pp.727,744, April 2003.

[7] Valenzuela, G.R., Theories for the interaction of electromagnetic and oceanic waves - a review. Boundary-Layer Meteorology, 13(1-4): 61–85, Jan. 1978.

[8] Elfouhaily, T.; Chapron, B.; Katsaros, K.; Vandemark, D., "A unified directional spectrum for long and short wind-driven waves,"J. Geophys. Res., vol. 102, no. C7, pp. 15 781–15 796, Jul. 1997.

[9] Soriano, G.; Guerin, C., "A Cutoff Invariant Two-Scale Model in Electromagnetic Scattering From Sea Surfaces," *Geoscience and Remote Sensing Letters, IEEE* , vol.5, no.2, pp.199,203, April 2008.

[10] Minchew, B., Determining the mixing of oil and sea water using polarimetric synthetic aperture radar, Geophys. Res. Lett., 39, L16607, 2012.

[11] Angelliaume, S.; Dubois-Fernandez, P.; Miegebielle, V.; Dubucq, D., "Polarimetric parameters for oil slicks detection using SAR data remote sensing — An evaluation," in *Geoscience and Remote Sensing Symposium (IGARSS), 2015 IEEE International* , vol., no., pp.3794-3797, 26-31 July 2015.

[12] Kudryavtsev, V.N.; Chapron, B.; Myasoedov, A.G.; Collard, F.; Johannessen, J.A., "On Dual Co-Polarized SAR Measurements of the Ocean Surface," *Geoscience and Remote Sensing Letters, IEEE* , vol.10, no.4, pp.761,765, July 2013.

[13] Angelliaume, S.; Fabbro, V.; Soriano, G.; Guerin, C.-A., "The GO-SSA Extended model for all-incidence sea clutter modeling," *Geoscience and Remote Sensing Symposium (IGARSS), 2014 IEEE International*, Quebec City, QC, 2014, pp. 5017-5020.

[14] Gregers-Hansen, V. and R. Mittal, "An improved empirical model for radar sea clutter reflectivity". IEEE Transaction on Aerospace and Electronic Systems, 2012. 48(4): p. 3512–3524.

[15] Minchew, B.; Jones, C. E.; Holt, B., "Polarimetric Analysis of Backscatter From the Deepwater Horizon Oil Spill Using L-Band Synthetic Aperture Radar," in *IEEE Transactions on Geoscience and Remote Sensing*, vol. 50, no. 10, pp. 3812-3830, Oct. 2012.

[16] Wismann et al. "Radar signatures of marine mineral oil spills measured by an airborne multi-frequency radar," *Int. J. Remote Sens.*, vol. 19, no. 18, pp. 3607–3623, 1998.

[17] Gade et al. "Imaging of biogenic and anthropogenic ocean surface films by the mul- tifrequency/multipolarization SIR-C/X-SAR," *J. Geophys. Res.*, vol. 103, no. C9, pp. 18 851–18 866, 1998.